J|A|C|S
COMMUNICATIONS

Synthesis of Cu−In−S Ternary Nanocrystals with Tunable Structure and Composition

Daocheng Pan,[†] Lijia An,[§] Zhongming Sun,[¶] William Hou,[‡] Yang Yang,[‡] Zhengzhong Yang,[*,#] and Yunfeng Lu[*,†]

Departments of Chemical Engineering and Materials Science Engineering, University of California, Los Angeles, California 90095, State Key Laboratory of Polymer Physics and Chemistry, Changchun Institute of Applied Chemistry, Chinese Academy of Sciences, Changchun 130022, China, Department of Physics, Washington State University, Richland, Washington 99354, and Institute of Chemistry, Chinese Academy of Sciences, Beijing, 10080 China

Received December 11, 2007; E-mail: luucla@ucla.edu

With increasing global energy consumption, fabricating low-cost, high-efficiency photovoltaic cells has emerged as a popular research direction. Compared with organic photovoltaic cells, an inorganic photovoltaic cell is generally more efficient but costs more to manufacture. Developing colloidal routes that enable low-cost fabrication of inorganic cells through a wet-chemistry process, such as spin-casting[1,2] and printing[3] of semiconductor nanocrystal colloidal solution, has therefore attracted a great deal of attention.[4,5]

This work reports the synthesis of ternary Cu−In−S nanocrystals, a class of materials suitable for high-efficiency solar cell fabrication. Generally, such ternary nanocrystals are synthesized by solid-state reaction,[6] solvothermal,[7−9] thermolysis,[10,11] or hot-injection technique.[12,13] It has been known that crystal structure, composition, and size of the nanocrystals may significantly affect their optoelectronic property and device performance.[14] Although the structure of nanocrystals can be generally controlled by the capping ligands used, as well as reaction conditions, the reported Cu−In−S nanocrystals are still limited to the chalcopyrite structure.[6−14] Moreover, composition of the current Cu−In−S nanocrystals is mainly controlled by using a single ternary precursor with a predesigned Cu−In−S ratio. Although the use of a single precursor source is convenient, this method is limited by the precursor availability and their tedious complicated synthesis procedure.[10,11]

Our synthesis strategy is to use mixed precursors that can be readily synthesized. Briefly, we used a hot-injection method based on $Cu(dedc)_2$ and $In(dedc)_3$ precursors, where dedc is diethyl dithiocarbamate. We used oleylamine as the activation agent and oleic acid or dodecanthiol as the capping agent. Judicious choice of the precursor ratio affords the nanocrystals with tunable [Cu]/[In] composition. Furthermore, appropriate choice of the capping agent allows precise control of the crystalline structure from zincblende to wurtzite (see Supporting Information for details). Similarly, tuning synthesis conduction and concentration of the capping agent allows us to control the nanoparticle size.

Figure 1 shows the XRD patterns of $CuInS_2$ nanocrystals prepared using oleic acid and dodecanethiol as the capping agents. We noticed that both the diffraction patterns do not match with those reported in the literature[6−14] or the standard JCPDS card database, which is mainly the patterns of tetragonal $CuInS_2$ (JCPDS 85−1575). We therefore simulated the diffraction patterns of

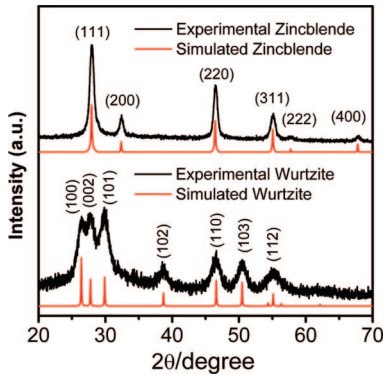

Figure 1. Experimental and simulated XRD patterns of $CuInS_2$ nanocrystals synthesized at 180 °C with a zincblende and a wurtzite structure.

zincblende and wurtzite $CuInS_2$ (see Supporting Information for details) and compared them with the experimental patterns. As shown in Figure 1, both simulated and experimental patterns are well matched, indicating these nanocrystals feature a zincblende and a wurtzite structure. To the best of our knowledge, this is the first report of the $CuInS_2$ nanocrystals with the zincblende and wurtzite structure.

It is important to mention that varying the Cu/In precursor ratio results in nanoparticles with similar diffraction patterns (see Figure S2), which is possibly due to the similar Cu^+ (0.74 Å) and In^{3+} (0.76 Å) radius. Moreover, on the basis of the different occupation probabilities of Cu, In, and S in a zincblende unit cell, the simulated patterns (Figure S2) of the $Cu_xIn_yS_{0.5x+1.5y}$ nanocrystals with a [Cu]/[In] ratio from 3/1 to 1/3 also show similar patterns with decreasing (200) and (222) reflection intensity. This observation is further consistent with the experimental results. The size of the nanocrystals calculated by the Scherrer equation shows an increasing tendency with the increase of the [Cu]/[In] ratio, also consistent with the TEM observation.

The composition of the nanoparticles was studied by energy dispersive spectroscopy (EDS) (Figure S3). Note that $Cd(dedc)_2$ and $Zn(dedc)_2$ have been used to synthesize CdS and ZnS nanocrystals by a thermolysis approach at high temperatures.[15,16] When used as the co-precursor, ternary nanoparticles with tunable composition can be readily achieved. Table 1 lists the quantitative analysis of the zincblende nanoparticles prepared with the [Cu]/[In] ratios ranged from 3/1 to 1/3, indicating that the composition of these nanoparticles is tunable and highly consistent with the formula $Cu_xIn_yS_{0.5x+1.5y}$. Note that using a higher [Cu]/[In] ratio of 1/3 leads to nanoparticles with Cu/In ratios around 1/2.2, possibly due to the difficulty in alloying the larger indium atoms. X-ray photoelectron spectrum (XPS, Figure S4) of representative

[†] Department of Chemical and Biomolecular Engineering, University of California, Los Angeles.
[‡] Department of Materials Science Engineering, University of California, Los Angeles.
[§] Changchun Institute of Applied Chemistry, Chinese Academy of Sciences.
[¶] Washington State University.
[#] Institute of Chemistry, Chinese Academy of Sciences.

Published on Web 04/09/2008

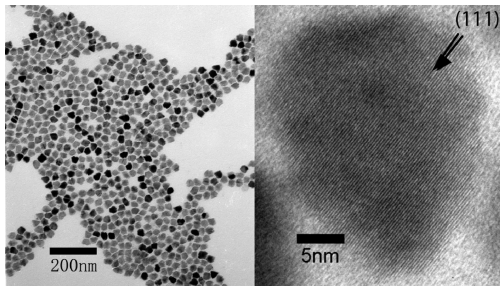

Figure 2. (Left) TEM and HR-TEM images (right) of zincblende $Cu_{1.0}In_{2.0}S_{3.5}$ nanocrystals synthesized at 250 °C.

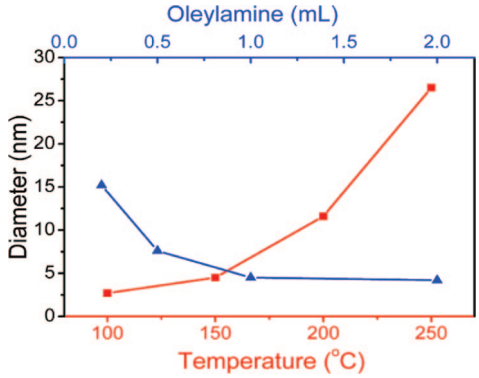

Figure 3. Tuning diameter of the zincblende nanocrystals $Cu_{1.0}In_{2.0}S_{3.5}$ by reaction temperature and controlling the amount of oleylamine added.

Table 1. Composition of the Zincblende $Cu_xIn_yS_{0.5x+1.5y}$ Nanocrystals and Their Formula

formula[a]	Cu%	In%	S%	formula[b]
$Cu_{3.0}In_{1.0}S_{3.0}$	42.10	14.03	43.87	$Cu_{3.0}In_{1.0}S_{3.1}$
$Cu_{2.0}In_{1.0}S_{2.5}$	35.25	17.64	47.10	$Cu_{2.0}In_{1.0}S_{2.7}$
$Cu_{1.0}In_{1.0}S_{2.0}$	26.21	23.54	50.25	$Cu_{1.1}In_{1.0}S_{2.1}$
$Cu_{1.0}In_{2.0}S_{3.5}$	16.41	30.39	53.20	$Cu_{1.0}In_{1.9}S_{3.2}$
$Cu_{1.0}In_{3.0}S_{5.0}$	14.36	31.28	54.35	$Cu_{1.0}In_{2.2}S_{3.8}$

[a] Calculated by the ratio of [Cu]/[In] precursor used. [b] Calculated by EDS.

$CuIn_2S_{3.5}$ nanocrystals shows that Cu_{2p} is split into $2p_{3/2}$ (933.0 eV) and $2p_{1/2}$ (952.4 eV), which is in good accordance with those reported.[17,18] These nanoparticles demonstrate good solubility in common solvents, such as hexane and toluene, which allows their processing through the simple casting or printing process. Figure S5 shows a UV/vis absorption spectrum of the zincblende $CuInS_2$ nanocrystals. The band gap of the $CuInS_2$ nanocrystals is calculated to be 1.45 eV, which is close to that of bulk $CuInS_2$ (1.50 eV), matching well with the AM1.5 solar spectrum. The inset of Figure S5 shows a photograph of $CuInS_2$ nanocrystals dispersed in toluene at room temperature, showing a black color due to their strong absorbance for visible light.

Besides the composition and structure control, size of the nanocrystals can also be tuned by adjusting the ratio of Cu/In precursor, reaction temperature, the concentration of activation agent, and capping agent. For example, with the increase of [Cu]/[In] ratios, the size of the zincblende $Cu_{1.0}In_{2.0}S_{3.5}$, $Cu_{1.0}In_{1.0}S_{2.0}$, $Cu_{2.0}In_{1.0}S_{2.5}$, and $Cu_{3.0}In_{1.0}S_{3.0}$ nanoparticles increases from 15, 21, 24, and 30 nm, respectively, while maintaining a narrow size distribution (Figure S6). Figure 3 illustrates the effects of reaction temperature and the amount of oleylamine used on the $Cu_{1.0}In_{2.0}S_{3.5}$ nanocrystal size. Clearly, increasing the reaction temperature for $Cu_{1.0}In_{2.0}S_{3.5}$ from 100 to 250 °C resulted in an increasing nanoparticle size from 2.8 to 27.0 nm estimated from TEM and the Scherrer equation (Figure S7). Note that oleylamine is an organic base that expedites the precursor decomposition at low temperature, and the copper and indium precursors could not decompose until 260 °C in the absence of oleylamine. A low oleylamine concentration results in less critical nuclei, leaving the majority of the precursors for nanocrystal growth in larger nanoparticles. As shown in Figure 3, the $Cu_{1.0}In_{2.0}S_{3.5}$ nanocrystals with size ranging from 4.2 to 15.2 nm could be obtained by simply adjusting the amount of oleylamine used (Figure S8). Compared with oleylamine, the capping agent forms stable complexes with the precursor or binds on the nanocrystal surface, which slows the nucleation and growth process. Therefore, a high oleic acid concentration results in less nucleus and thus larger nanocrystals, although its effect is less significant than that of oleylamine (see Figure S9).

Figure 2a shows a TEM image of the zincblende $Cu_{1.0}In_{2.0}S_{3.5}$ nanocrystals synthesized at 250 °C (see SAED in Figure S2). Narrowly distributed nanoparticles with an average diameter of 28.6 nm and a standard deviation of 7.4% are observed, which are very close to the size calculated from XRD. High-resolution TEM image (Figure 2b) indicates that these nanoparticles are single crystalline. The formation of such nanoparticles may involve the reactions of CuS or Cu_2S decomposed from $Cu(dedc)_2$ with In_2S_3 decomposed from $In(dedc)_3$ in the presence of oleic acid or dodecanethiol (see Supporting Information for details).

In summary, nearly monodisperse Cu−In−S ternary semiconductor nanocrystals with tunable [Cu]/[In] composition, crystalline structure, and particles size were synthesized by a hot-injection approach using mixed generic precursors. Moveover, ternary Cu−In−S nanocrystals with tunable zincblende and wurtzite structure were reported for the first time. This work correlates the crystalline structure of the binary ZnS nanoparticles with those of the ternary Cu−In−S nanocrystals, demonstrating the feasibility of fabricating their alloyed or core/shell structures. For the long run, this work may provide suitable material candidates for low-cost, high-efficiency solar cell fabrication. More systematic work on preparing binary/ternary core/shell structure and alloys, as well as device integration, is underway.

Acknowledgment. This work was partially supported by ONR, NSF-CAREER, and Sandia National Laboratories.

Supporting Information Available: Detailed information on nanocrystal preparation and characterization, EDS, TEM, XRD, UV−vis, XPS spectra, and formation mechanism. This material is available free of charge via the Internet at http://pubs.acs.org.

References

(1) Gur, I.; Fromer, N. A.; Geier, M. L.; Alivisatos, A. P. *Science* **2005**, *310*, 462.
(2) Huynh, W. U.; Dittmer, J. J.; Alivisatos, A. P. *Science* **2002**, *295*, 2425.
(3) Kay, A.; Gratzel, M. *Sol. Energy Mater. Sol. Cells* **1996**, *44*, 99.
(4) Murray, C. B.; Norris, D. J.; Bawendi, M. G. *J. Am. Chem. Soc.* **1993**, *115*, 8706.
(5) Peng, Z. A.; Peng, X. G. *J. Am. Chem. Soc.* **2001**, *123*, 183.
(6) Yoshino, K.; Ikari, T.; Shirakata, S.; Miyake, H.; Hiramatsu, K. *Appl. Phys. Lett.* **2001**, *78*, 742.
(7) Xiao, J.; Xie, Y.; Xiong, Y.; Tang, R.; Qian, Y. T. *J. Mater. Chem.* **2001**, *11*, 1417.
(8) Li, B.; Xie, Y.; Huang, J.; Qian, Y. T. *Adv. Mater.* **1999**, *11*, 1456.
(9) Jiang, Y.; Wu, Y.; Mo, X.; Yu, W. C.; Xie, Y.; Qian, Y. T. *Inorg. Chem.* **2000**, *39*, 2964.
(10) Castro, S. L.; Bailey, S. G.; Raffaelle, R. P.; Banger, K. K.; Hepp, A. F. *J. Phys. Chem. B* **2004**, *108*, 12429.
(11) Castro, S. L.; Bailey, S. G.; Raffaelle, R. P.; Banger, K. K.; Hepp, A. F. *Chem. Mater.* **2003**, *15*, 3142.
(12) Malik, M. A.; O'Brien, P.; Revaprasadu, N. *Adv. Mater.* **1999**, *11*, 1441.
(13) Zhong, H. Z.; Li, Y. C.; Ye, M. F.; Zhu, Z. Z.; Zhou, Y.; Yang, C. H.; Li, Y. F. *Nanotechnology* **2007**, *18*, 025602.
(14) Qiu, J. J.; Jin, Z. G.; Wu, W. B.; Xiao, L. *Thin Solid Films* **2006**, *510*, 1.
(15) Ludolph, B.; Malik, M. A.; O'Brien, P.; Revaprasadu, N. *Chem. Commun.* **1998**, 1849.
(16) Malik, M. A.; Revaprasadu, N.; O'Brien, P. *Chem. Mater.* **2001**, *13*, 913.
(17) Muller, K.; Milko, S.; Schmeiber, D. *Thin Solid Films* **2003**, *431−432*, 312.
(18) Xiao, J. P.; Xie, Y.; Tang, R.; Qian, Y. T. *J. Solid State Chem.* **2001**, *161*, 179.

JA711027J